Distinct Membrane Domains on Endosomes in the Recycling Pathway Visualized by Multicolor Imaging of Rab4, Rab5, and Rab11✪

Birte Sönnichsen,* Stefano De Renzis,* Erik Nielsen,* Jens Rietdorf,‡ and Marino Zerial*

*Max Planck Institute for Molecular Cell Biology and Genetics, 01307 Dresden, Germany; and ‡Advanced Light Microscopy Facility, European Molecular Biology Laboratory, 69117 Heidelberg, Germany

Abstract. Two endosome populations involved in recycling of membranes and receptors to the plasma membrane have been described, the early and the recycling endosome. However, this distinction is mainly based on the flow of cargo molecules and the spatial distribution of these membranes within the cell. To get insights into the membrane organization of the recycling pathway, we have studied Rab4, Rab5, and Rab11, three regulatory components of the transport machinery. Following transferrin as cargo molecule and GFP-tagged Rab proteins we could show that cargo moves through distinct domains on endosomes. These domains are occupied by different Rab proteins, revealing compartmentalization within the same continuous membrane. Endosomes are comprised of multiple combinations of Rab4, Rab5, and Rab11 domains that are dynamic but do not significantly intermix over time. Three major populations were observed: one that contains only Rab5, a second with Rab4 and Rab5, and a third containing Rab4 and Rab11. These membrane domains display differential pharmacological sensitivity, reflecting their biochemical and functional diversity. We propose that endosomes are organized as a mosaic of different Rab domains created through the recruitment of specific effector proteins, which cooperatively act to generate a restricted environment on the membrane.

Key words: endocytosis • transferrin recycling • Rab proteins • EEA1

Introduction

Eukaryotic cells internalize components from the extracellular medium via endocytosis (Gruenberg and Maxfield, 1995; Mellman, 1996). Organelles within the endosomal membrane system have been mainly defined following the flow of different cargo molecules. All internalized molecules are transported to early endosomes, also called sorting endosomes (Dunn et al., 1989). These membranes, scattered throughout the cell periphery, are filled with cargo within two to five minutes after internalization (Besterman et al., 1981; Griffiths et al., 1989). Here most ligands dissociate from their cognate receptors and are, together with fluid phase material, delivered to late endosomes and lysosomes for degradation. Receptors, such as the transferrin receptor, are often recycled for a new round of internalization (Hopkins, 1983; Dunn et al., 1989). The bulk of transferrin is returned to the surface with a half-time of three to five minutes (Schmid et al., 1988; Mayor et al., 1993). The remaining fraction accumulates in membranes that comprise of tubular vesicular structures located in the vicinity of the microtubule organizing center (Hopkins, 1983; Yamashiro and Maxfield, 1984). Since these membranes do not receive material destined for late endosomes and lysosomes (Ghosh et al., 1994), and their pH is slightly higher than that of early endosomes (Yamashiro and Maxfield, 1984; Sipe and Murphy, 1987), they were defined as a distinct organelle, the pericentriolar recycling endosome.

Considering the structural and functional properties of endosomes, several problems arise for the distinction of these two membrane pools by cargo accessibility and morphological criteria. First, the flow of cargo through endosomes becomes increasingly asynchronous with time. Second, the spatial separation between early and recycling endosomes is not apparent in all cell types. For example, transferrin-accumulating membranes are more concentrated around the microtubule organizing center in CHO cells than in A431 cells. Third, endosomal membranes are extremely pleomorphic (Griffiths et al., 1989) and their morphology varies between cell types (Hopkins et al., 1990; Yamashiro and Maxfield, 1984). Carrier vesicles for

✪The online version of this paper contains supplemental material.

Address correspondence to Birte Sönnichsen or Marino Zerial, European Molecular Biology Laboratory, Meyerhofstrasse 1, 69117 Heidelberg, Germany. E-mail: sonnichs@embl-heidelberg.de or zerial@embl-heidelberg.de

Drs. Sönnichsen, De Renzis, Nielsen, and Zerial's current address is c/o European Molecular Biology Laboratory, 69117 Heidelberg, Germany.

recycling cargo have not been characterized. Consequently, by the so far applied criteria, tubules and vesicles of the recycling endosome cannot be distinguished from transport intermediates.

A more accurate definition of endosomal organelles must therefore include their molecular machinery. Early and recycling endosomes are at the crossroad of several transport routes. They continuously exchange membrane with late endocytic compartments, the plasma membrane, and the TGN (Ghosh et al., 1998), and, in addition, undergo homotypic fusion and fission reactions. All these trafficking events tend to average the biochemical composition over time. How can endosomes then maintain their functional identity?

A group of regulatory molecules localized to distinct subsets of membranes along the secretory and endocytic pathway are members of the Rab family of small GTPases (Pfeffer, 1994; Novick and Zerial, 1997). In the GTP-bound state Rab proteins recruit specific effector proteins to the membrane. These have multiple functions, ranging from membrane budding (McLauchlan et al., 1998) or docking (Christoforidis et al., 1999a; Guo et al., 1999) to interactions with the cytoskeleton (Echard et al., 1998; Nielsen et al., 1999). Interference with their GTPase cycle provokes drastic morphological and functional changes in the target organelles, suggesting that Rab proteins contribute to the organization of membranes. One of the best-studied Rab proteins on endosomes is Rab5. It is required for the delivery of material from the plasma membrane to early endosomes as well as homotypic endosome fusion (Gorvel et al., 1991; Bucci et al., 1992; McLauchlan et al., 1998). We recently identified a surprisingly large number of cytosolic proteins binding specifically to the activated form of Rab5 (Christoforidis et al., 1999a). Rather than serving completely distinct functions, these Rab5 effectors appear to act cooperatively. Upon activation by the Rabaptin-5/Rabex-5 complex (Horiuchi et al., 1997), Rab5 can recruit phosphoinositol-3 kinases (Christoforidis et al., 1999b), including hVPS34 (Schu et al., 1993), ensuring the local generation of phosphoinositol-3-phosphate (PI(3)P)[1]. An environment of PI(3)P and active Rab5 is essential for the binding of the docking protein EEA1 (early endosomal antigen 1) to the endosomal membrane (Patki et al., 1997; Mills et al., 1998; Simonsen et al., 1998; Christoforidis et al., 1999a). EEA1 itself directly interacts with the SNARE syntaxin13 in a dynamic, oligomeric complex (McBride et al., 1999).

Rab5 can therefore be seen as a regulatory anchor for factors that create a restricted, fusion competent domain on the early endosome (McBride et al., 1999). This working model can explain how endosomes might be organized to sustain extensive membrane exchange without compromising their structural and functional integrity. If generalized for other family members, the model would predict that Rab proteins with their specific set of effectors can contribute to a compartmentalization within a continuous membrane structure. A functional arrangement of machineries controlling vesicle targeting, protein sorting or cytoskeletal interactions into domains would help to increase the efficiency and coordination of these processes.

[1]*Abbreviations used in this paper:* EEA1, early endosomal antigen 1; PI(3)P, phosphoinositol-3-phosphate; VSV-G, vesicular stomatitis virus glycoprotein.

Apart from Rab5, two other Rab proteins have been implicated in the recycling pathway, Rab4 and Rab11. Rab4 was suggested to play a role in fast recycling from early endosomes back to the plasma membrane (Van der Sluijs et al., 1992, Sheff et al., 1999). Rab11 has been localized to the recycling endosome, the TGN and specialized storage membranes of regulated secretory pathways (Urbe et al., 1993; Ullrich et al., 1996; Jedd et al., 1997; Calhoun et al., 1998). Mutants of Rab11 effect transferrin recycling (Ullrich et al., 1996; Ren et al., 1998) and transport of vesicular stomatitis virus glycoprotein (VSV-G) to the plasma membrane (Chen et al., 1998). Our model would predict that Rab4 and Rab11 should be enriched in membrane domains distinct from that of Rab5, but that can reside on the same endosome. Could different arrangements of these domains account for morphologically and kinetically distinct transferrin recycling structures?

To test this hypothesis we have visualized Rab4, Rab5, and Rab11 in combination with endosomal cargo. Our results provide evidence for the proposed domain organization of endosomes.

Materials and Methods

Cell Lines and Antibodies

A431 cells were grown in DME supplemented with 10% (vol/vol) FCS, 100 U/ml penicillin, 100 μg/ml streptomycin, and 2 mM L-glutamine. Rab proteins were fused COOH-terminally to GFP using the pEGFP-C3, pECFP-C3, or pEYFP-C3 vectors provided by CLONTECH Laboratories, Inc. Stable cell lines were selected and maintained in medium containing 0.5 mg/ml G418 (Sigma-Aldrich). Polyclonal rabbit antibodies against Rab11 were raised and affinity purified against recombinant protein. mAbs against transferrin receptor (H68.4) were obtained from Zymed Laboratories. Polyclonal rabbit TGN46 antiserum was kindly provided by V. Ponnambalam (University of Dundee, UK), human polyclonal EEA1 antibodies by H. Stenmark (University of Oslo, Norway), and affinity-purified rabbit polyclonal antibody against GFP by N. Le Bot (EMBL, Heidelberg, Germany).

Biochemical Transferrin Recycling Assay

Iron-saturated human transferrin and iron-saturated biotin-labeled transferrin were purchased from Sigma-Aldrich.

A431 cells were serum starved for 2 h to deplete endogenous transferrin. Biotinylated transferrin was internalized at 10 μg/ml for 2 min at 37°C.

Unbound and surface-bound transferrin was removed by washing the cells with ice-cold PBS containing 1 mg/ml unlabeled transferrin followed by low pH buffer (150 mM NaCl, 10 mM acetic acid, pH 3.5, and 1 mg/ml unlabeled transferrin). This procedure resulted in the removal of 95–98% of surface-bound ligand. To measure recycling, cells were returned to 37°C in the presence of 1 mg/ml of unlabeled transferrin. At each time point the medium was collected, cells were washed with ice-cold PBS and homogenized in 1 ml of lysis buffer (PBS containing 2% Triton X-100 and 0.4% SDS). 5 μl of the supernatant (recycled biotinylated transferrin), or 5 μl of the lysate (cell-associated biotinylated transferrin) were quantified as described previously (Zacchi et al., 1998). Results were expressed as percent of the total signal.

Internalization of Fluorescently Labeled Transferrin and Immunofluorescence

A431 cells were grown on glass coverslips and serum starved for 1 h before incubation with 60 μg/ml fluorescently labeled transferrin (Molecular Probes). The probe was chased in the presence of a fivefold excess of nonlabeled transferrin.

Immunofluorescence labeling was performed according to standard procedures. Antibodies against transferrin receptor and TGN46 were diluted 1/100, EEA1 antiserum was used at 1/500, Rab11 antibody at 1/200 dilution. Cells were mounted in ProLong™ Antifade (Molecular Probes).

Incubations with 5 μg/ml brefeldin A (Sigma-Aldrich) or 50–100 nM wortmannin (Sigma-Aldrich) were performed in serum-free medium.

Microinjection

Plasmid DNAs encoding the Rab proteins were injected into the cell nucleus using an Eppendorf micromanipulator and transjector. Compared with transient transfections, we found that this technique ensured a better control over expression levels in general and a constant ratio of the two fusion proteins in particular. Expression of the CFP was generally lower compared with the YFP fusion proteins. A mixture of 7 ng/μl YFP and 20 ng/μl CFP plasmid DNA when monitored 6–14 h after injection resulted in similar expression levels as seen in the stable cell lines.

Live Cell Imaging

Cells were grown on life cell imaging dishes (MatTek Corp.). Imaging was performed in CO_2-independent medium (GIBCO BRL). Time-lapse series were acquired at 37°C on an inverted Olympus IX70 microscope, equipped with a 100× oil immersion objective, NA 1.35, and a 12-bit Till Imago CCD camera (Till Photonics). The temperature was controlled by a climate box covering the set up. Filters (AHF Analysentechnik) allowed for simultaneous detection of CFP and YFP or GFP and rhodamine, respectively. Switching between the excitation wavelengths with a Polychrome II multiwavelength illumination system was controlled by the TillvisION 3.3 software (Till Photonics). Exposure times were 200–300 ms for each channel followed by a 60-ms readout delay, resulting in time-lapse sequences of roughly two frames per second, which were merged as RGBs using TILLvisION. Series were exported as single TIFF files, processed in Adobe Photoshop 5.0 or converted into QuickTime movies using IPLab 3.2 (Scanalytics Inc.).

Confocal Microscopy, Image Processing, and Quantitation of Signal Overlap on Fixed Cells

Images were acquired on the Compact Confocal Camera (CCC) as described by White et al., 1998, using a 63× 1.4 NA Plan-Apochromat III DIC objective (Carl Zeiss). Fluorescent dyes were imaged sequentially in frame-interlace mode to eliminate cross talk between the channels. CFP was excited with a 430-nm laser line (Directly Doubled Diode/D3; Coherent) and imaged through a combination of 440–505-nm bandpass and 525-nm longpass emission filters. YFP was exited with the 514-nm Argon laser line and imaged through a 525-nm longpass emission filter. Texas red was excited with the 594-nm Helium Neon laser line and imaged through a 610-nm longpass emission filter.

Serial sections were acquired satisfying the Nyquist criteria for sampling and processed on a multiprocessor SGI Unix computer using the Huygens System 2.2 (Scientific Volume Imaging BV). A maximum likelihood estimation (MLE)-based algorithm was used for image reconstruction. Z-stacks of images were exported as TIFF files, and individual sections were analyzed for fluorescent signal overlap by visual inspection. Using Adobe Photoshop 5, a 5 × 5-cm grid was projected onto the image of the reference channel, and in every second grid square all fluorescent structures were marked on a separate, superimposed layer. Signals were referred to as individual structures if they comprised of a continuous patch of intensity values >50 (in a range of 0–255). This layer was then projected onto the corresponding images for the other two channels, and the underlying image was analyzed for fluorescent signal at the marked position. At least two sections per cell were counted, ensuring that peripheral and perinuclear structures were equally taken into account. 5–10 cells were analyzed, counting 150–200 fluorescent structures per cell.

Electron Microscopy

A431 cells stably expressing Rab4- or Rab5-GFP were labeled with BSA-gold (5 nm) at an OD(520) of 0.5. Cells were washed extensively and harvested with a cell scraper. After homogenization (3 mM imidazole, pH 7.4, 250 mM sucrose, 2 mM $MgCl_2$) with a 22.5-gauge needle, unbroken cells and nuclei were sedimented at 1,000 *g* for 10 min. The resulting PNS was supplemented with an ATP regenerating system (10 mM ATP, 80 mM creatine phosphate, 0.4 mM creatine kinase) and 1 mM GTP and incubated with carbon-coated copper grids at room temperature for 15 min. After fixation with 2% (wt/vol) paraformaldehyde for 10 min, unspecific binding sites and remaining fixative were blocked with 0.8% (wt/vol) BSA, 0.1% (vol/vol) fish skin gelatin, and 20 mM glycine in PBS for 10 min. Antibodies against EEA1, GFP, and Rab11 were diluted in blocking solution at 1:50, 1:200, and 1:30, respectively. Protein A conjugated to 10-nm gold was diluted according to the manufacturer's instructions (Slot and Geuze, University of Utrecht). The first antibody/protein A complex was fixed with 1% (vol/vol) glutaraldehyde in PBS for 10 min. After quenching of the fixative with 20 mM glycine in PBS, the immunolabeling procedure was repeated with the second antibody and protein A conjugated to 15-nm gold. Finally, the material was stained with 2% methyl cellulose and 3% uranyl acetate in a mixture of 1:3 for 5 min at 4°C. Specimen were observed on a Philips CM120 BioTwin transmission electron microscope.

For quantitation, random images of membrane-containing fields were taken at 27,000 magnification. Endosomes were identified by the internalized BSA-gold. 50–100 endosomes on ten images were analyzed for immunogold labeling, and the results were expressed as a percentage of the total identified endosomes.

Online Supplemental Material

All videos were acquired and processed as described previously in Live Cell Imaging. They comprise 40–60 frames, animated at 10 frames/s (~10× acquisition speed). The videos can be found at http://www.jcb.org/cgi/content/full/149/4/901/DC1.

Movies 1–3. Rab4, Rab5, and Rab11 occupy subdomains on transferrin-labeled endosomes.

Movie 1. A431 cell expressing GFP-Rab5 after 10 min internalization of rhodamine transferrin. Note that transferrin (red) frequently enters tubules that do not contain Rab5 (green), but seem to be connected with the more globular Rab5 structures. In the center, a segregation event of Rab5 from a larger transferrin-filled endosome can be observed.

Movie 2. A431 cell expressing GFP-Rab4 after 10 min internalization of rhodamine transferrin followed by a 5-min chase. Note the tubules and small vesicles extending from larger structures that contain both Rab4 (green) and transferrin (red).

Movie 3. A431 cell expressing GFP-Rab11 after 10 min internalization of rhodamine transferrin followed by a 30-min chase. Transferrin (red) and Rab11 (green) containing structures have accumulated in the pericentriolar area. Note though, that also on transferrin-labeled structures located more in the periphery Rab11 occupies vesicular and tubular subdomains.

Movies 4–6. Rab4, Rab5, and Rab11 occupy subdomains that can be located on the same endosome.

Movie 4. A431 cell coexpressing YFP-Rab4 and CFP-Rab5. Three populations of membranes can be observed: two, which have either only Rab4 (green) or only Rab5 (red), and a third containing both, as shown by the yellow color in the overlapping regions. Note that Rab4 and Rab5 do not completely overlap; in contrast, they are often segregated into different domains on these structures.

Movie 5. In A431 cells coexpressing CFP-Rab5 and YFP-Rab11 little overlap is observed between the small vesicular and tubular Rab11 structures (green) and the bigger globular Rab5 endosomes (red). However, both kinds of membranes are often located in close proximity.

Movie 6. In A431 cells coexpressing YFP-Rab4 and CFP-Rab11 a significant population of endosomes contains both Rab4 (red) and Rab11 (green). However, again little yellow overlap is observed, both proteins occupy mostly separate domains on the same membrane (compare video 4).

Movies 7–9. Differential response of Rab4/5 and Rab4/11 endosomes to treatment with brefeldin A.

Movie 7. A431 cell expressing GFP-Rab4 (green) after internalization of rhodamine transferrin (red) for 10 min followed by incubation with 5 μg/ml BFA for 10 min. Note the dynamics of the extensive tubular network containing both Rab4 and transferrin, but also the remaining globular endosomes that seem to have transient interactions with the network.

Movie 8. In A431 cells coexpressing YFP-Rab4 and CFP-Rab11 both proteins are found in the tubular network generated after 10 min of BFA treatment. Note though, that a significant population of Rab4 (red) remains in globular endosomes that do not contain Rab11.

Movie 9. A431 cells coexpressing YFP-Rab4 and CFP-Rab5 demonstrate that endosomes containing Rab5 (red) do not enter the tubular network caused by treatment with BFA. Rab4 (green) can be found on Rab5 structures and on tubules that seem to form transient connections with the globular Rab4/Rab5 endosomes.

Movie 10. A431 cell coexpressing YFP-Rab4 and CFP-Rab5. Rab5 endosomes (red) tubulate in response to treatment with 100 nM wortmannin for 30 min.

Results

GFP Fusion Proteins of Rab4, Rab5, and Rab11 Are Correctly Localized to Their Target Membranes

To demonstrate that endosomal membrane organization visualized via GFP fusion proteins reflects the situation in normal cells, we had to establish that the expressed Rab proteins were correctly localized and did not alter the transferrin cycle. Using human A431 cells in which transferrin recycling has been extensively characterized (Hopkins, 1983), we generated stable cell lines expressing wild-type GFP-Rab4, -Rab5, or -Rab11. Overexpression was moderate, about fivefold over the endogenous levels as estimated by Western blotting (not shown). All three fusion proteins became membrane bound (Fig. 1) and could be extracted into the soluble pool by microinjected recombinant Rab GDI (GDP dissociation inhibitor) or by incubation with Rab GDI after permeabilization with streptolysin O (not shown). The GFP-Rab5 cell line has been described elsewhere (Nielsen et al., 1999). GFP-Rab5 was colocalizing with its effector EEA1, indicating that the GFP tag did not interfere with its correct membrane targeting (Fig. 1 A). GFP-Rab4 localized to endosomes, as defined by the presence of transferrin receptor (Fig. 1 C). Colocalization of GFP-Rab4 with EEA1 was often partial (compare Fig. 1, A with B). GFP-Rab11 labeling was found in the pericentriolar area as well as on small vesicular structures throughout the cytoplasm. These vesicles were distinct, but often in close proximity to EEA1-containing endosomes (Fig. 1 D). As previously demonstrated by antibody staining (Ullrich et al., 1996), the pericentriolar membranes colocalized partially with transferrin receptor (Fig. 1 E) and with a marker for the TGN, TGN46 (Fig. 1 F).

To measure transferrin recycling, biotinylated transferrin was internalized for 2 min at 37°C and chased in the presence of nonlabeled transferrin for up to 30 min (Fig. 1 G). Comparing wild-type A431 cells to all three cell lines, we found no major differences in the amounts of transferrin recycled to the medium. As previously noted (Van der Sluijs et al., 1992), expression of Rab4-GFP led to a slight increase in the early rates of recycling. After this initial characterization, we concluded that the GFP fusion proteins of Rab4, Rab5, and Rab11 could faithfully represent their endogenous counterparts in A431 cells.

Transferrin Travels through Rab5-, Rab4-, and Rab11-labeled Domains on Endosomes

We then followed the passage of transferrin through endosomes with respect to the machinery represented by Rab4, Rab5, and Rab11. In cells expressing GFP-Rab4, Rab5, or Rab11, rhodamine transferrin was internalized for 2 min at 37°C and chased in the presence of nonlabeled transferrin (Fig. 2 A). After fixation, images were acquired and overlap of fluorescent signal was quantified (see Materials and Methods). Early after internalization, the major population of transferrin-labeled structures (70%) colabeled with Rab5 (Fig. 2, A and B). This association was transient

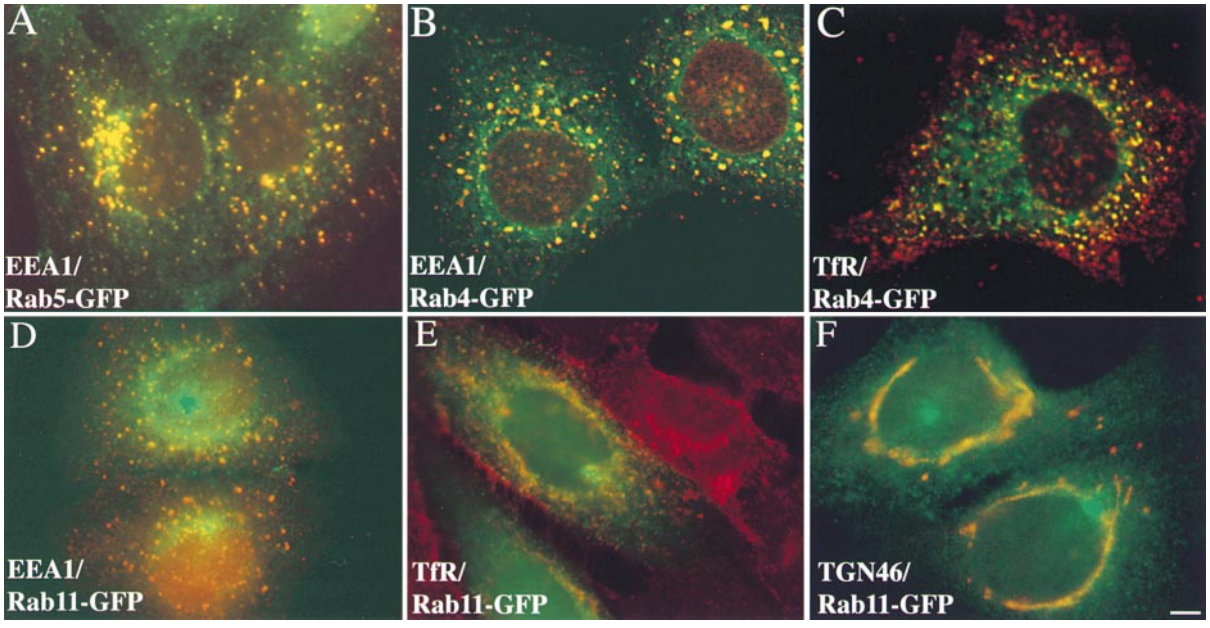

Figure 1. Characterization of A431 cell lines expressing GFP-Rab4, Rab5 or Rab11. A431 cells stably expressing GFP-Rab5 (A), GFP-Rab4 (B and C) or GFP-Rab11 (D, E, and F) were labeled with antibodies against EEA1 (A, B and D), transferrin receptor (C and E) or TGN46 (F) followed by secondary antibodies coupled to rhodamine. Images represent individual confocal sections. (G) Wild-type A431 cells and stable cell lines were labeled with biotinylated transferrin for 2 min at 37°C, followed by incubation in the presence of an excess of nonlabeled transferrin for the indicated time periods. Medium and cells were collected, and analyzed for biotinylated transferrin. Recycled transferrin was expressed as a percentage of the total. Bar, 2 μm.

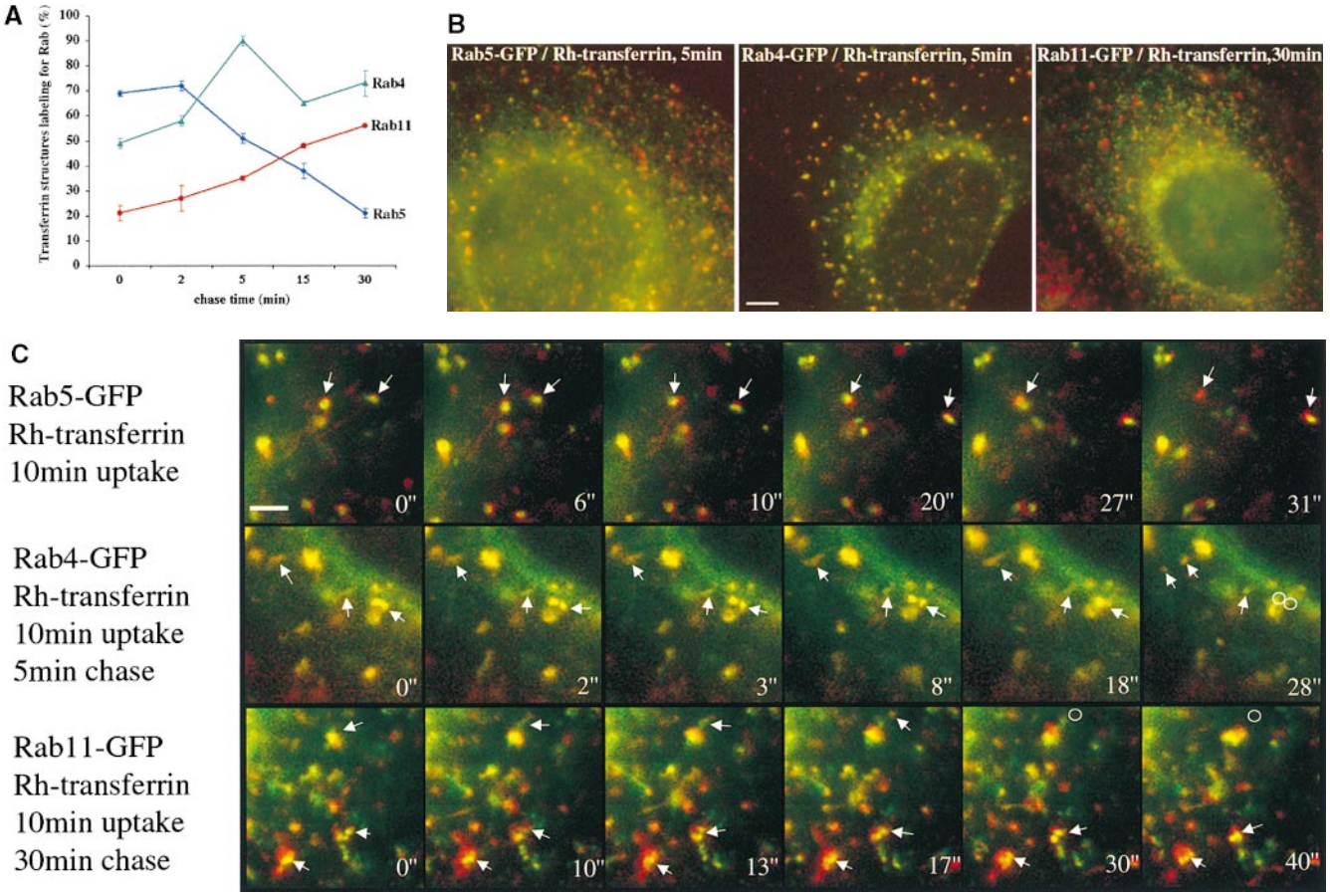

Figure 2. Time course for association of rhodamine transferrin with GFP-Rab4–, -Rab5–, or -Rab11–labeled endosomes in fixed and living cells. (A and B) A431 cells stably expressing GFP-Rab4 (triangles), GFP-Rab5 (diamonds), or GFP-Rab11 (circles) were labeled with rhodamine transferrin for 2 min at 37°C, followed by a chase for the indicated time periods. Images of fixed cells were analyzed for fluorescent overlap (see Materials and Methods). (A) Percentage of transferrin endosomes labeling for GFP-Rab proteins at the indicated time points. $n = 4–5$ cells. (B) Representative merged images for different time points. (C) Consecutive video images from time-lapse series of A431 cells stably expressing Rab5 (top), Rab4 (middle) or Rab11 (bottom) after internalization of rhodamine transferrin. Bars: (B) 2 μm; (C) 1 μm.

and decreased rapidly after the first minutes. The number of transferrin-labeled endosomes containing Rab11 increased slowly from ~20 to 55% during a 30-min chase (Fig. 2, A and B), in line with an involvement of Rab11 in late stages of recycling (Ullrich et al., 1996; Ren et al., 1998). Rab4 has been implicated in the fast route of recycling (Van der Sluijs et al., 1992; Sheff et al., 1999). Consistently, >90% of transferrin-labeled membranes contained Rab4 after a 5-min chase (Fig. 2, A and B). Surprisingly, ~70% remained positive for Rab4 at late time points (15 and 30 min after internalization) when >80% of the transferrin had been recycled (compare with Fig. 1 G), suggesting that a requirement for Rab4 might not be limited to early stages.

Early endosomes are comprised of globular and tubulovesicular membrane elements, which have been proposed to reflect different functional domains (Mayor et al., 1993). We hypothesized that if Rab proteins generate distinct domains on the membrane, Rab4, Rab5, and Rab11 might be differentially localized to these membrane elements. Strikingly, visualizing endosomes by time-lapse video microscopy we could distinguish distinct subdomains of GFP-Rab protein on larger transferrin-filled structures (Fig. 2 C and videos 1–3, transferrin in red, Rab proteins in green). Rab5 was mostly restricted to globular domains, and largely excluded from tubules and vesicles. Rapid segregation of transferrin from these Rab5-positive domains could frequently be observed (Fig. 2 C, arrows, and video 1). Both, Rab4 and Rab11 were seen on tubules and small globular domains forming on larger transferrin-labeled structures (Fig. 2 C, arrows, videos 2 and 3). Whereas Rab11 structures localized preferentially towards the cell center, those positive for Rab4 were more widely distributed. Tubules often fragmented into smaller, vesicular profiles (Fig. 2 C and video 3). In summary, these experiments suggested that Rab4, Rab5, and Rab11 are localized to discrete domains on endosomes.

Rab4, Rab5, and Rab11 Label Distinct Domains on the Same Endosomes

We next asked whether Rab4, Rab5, and Rab11 were differentially localized to domains of the same endosome. In other words, were Rab5 negative tubules that emerged

Table I. Quantitation of Rab4, Rab5, and Rab11 on Transferrin-labeled Early Endosomes

	Rab5	Rab4	Overlap
Tf endosomes, 30 min internalization	51.5 ± 8	79 ± 4	23.5 ± 7
Tf endosomes, 2 min internalization, 3 min chase	66 ± 6	68 ± 1	51 ± 8
Tf endosomes, 30 min internalization, 50 nM wortmannin	81 ± 9	54 ± 4	47 ± 14
	Rab5	Rab11	Overlap
Tf endosomes, 30 min internalization	54 ± 3	65 ± 1	19 ± 8
Tf endosomes, 30 min internalization, 50 nM wortmannin	88 ± 5	35 ± 1	30 ± 7
	Rab4	Rab11	Overlap
Tf endosomes, 30 min internalization	84 ± 1	68 ± 4	63.5 ± 5
Tf endosomes, 30 min internalization, 50 nM wortmannin	55.5 ± 2	34 ± 6	35 ± 6

Fluorescence analysis: Combinations of two different Rab proteins fused to YFP or CFP were expressed, and Texas red–labeled transferrin was internalized for the indicated time. Numbers represent the percentage of total transferrin-labeled endosomes positive for one or more Rab proteins.

from a transferrin-labeled endosome occupied by Rab4 or Rab11? To address this question, combinations of CFP and YFP fusions of the three Rab proteins were coexpressed in A431 cells. Texas red transferrin was internalized for 30 min to reach steady state labeling. After fixation, confocal serial sections were obtained and processed with a deconvolution software before quantification of overlapping fluorescent signals. Single endosomes were defined as structures with continuous transferrin signal (see Materials and Methods).

Interestingly, although residing on the same structure, as defined by the continuous labeling for transferrin, the fluorescent signals for the individual Rab proteins were mostly segregated (Fig. 3, insets). This suggested that Rab4, Rab5, and Rab11 could indeed occupy distinct domains on continuous membranes. Transferrin traverses through Rab5-positive endosomes early after internalization (Fig. 2 A). Consistently, at steady state the cargo was mainly found in Rab4 and Rab11 containing membranes (Fig. 3 and Table I). Remarkably, the majority (63 ± 5%) of these transferrin structures harbored both Rab4 and Rab11. In contrast, only about a quarter of the transferrin positive endosomes contained Rab4 and Rab5 (23.5 ± 7%, Fig. 3 and Table I). The lowest overlap was seen for Rab5 and Rab11 (19 ± 8%). The time course suggested that after leaving Rab5 endosomes, transferrin rapidly reached Rab4-positive membranes (Fig. 2 A). We therefore speculated that this transit might occur within the same endosomes containing both Rab4 and Rab5. Consistently, when we analyzed cells shortly after internalization, more than twice as many transferrin-filled endosomes contained Rab4 and Rab5, compared with the steady state situation (51 ± 8% vs. 23.5 ± 7%, Table I). This suggests that the cargo could be sorted from a Rab5 into a Rab4 domain, residing on the same membrane.

So far, we had confirmed that cargo-filled endosomes are structured in domains, represented by different Rab proteins. However, with this approach we could not determine whether in respect to the Rab machinery the composition of endosomes changes as transferrin flows through or whether cargo is transported between endosomes with a stable composition. If Rab proteins were subjected to a similar flow as cargo this should be reflected in a change of overlapping distribution between Rab4, Rab5, and Rab11 at different stages of recycling. To visualize all three Rab proteins together we detected endogenous Rab11 by antibody staining in cells coexpressing CFP-Rab5 and YFP-Rab4 (Fig. 3). All endosomes labeled for a particular Rab protein were counted and the extent of overlap with the other Rab proteins was determined at steady state and early after transferrin internalization. Under both conditions, half of the Rab4-positive endosomes also contained Rab5, suggesting a relatively stable pool of membranes with this composition (Table II). Another pool, similar in size, contained Rab4 and Rab11, and a quarter of the Rab4 endosomes was positive for all three Rab proteins. Interestingly, whereas most of the Rab4 structures colocalized either with Rab5 or Rab11 or both, about half the population of Rab5-positive endosomes did not label for either of the other Rab proteins (Table II).

Taken together, the quantification suggests that transferrin moves through endosomes that are structured in domains labeling for Rab5, Rab4, or Rab11. Via membranes that are mainly Rab5-positive, the cargo enters a pool of endosomes that contain both Rab5 and Rab4. Transfer from this pool is fast, and at steady state transferrin is

Table II. Quantitation of Rab4, Rab5, and Rab11 Overlap on the Same Endosomes

	Rab5 only	Rab4 and 5	Rab5 and 11	Rab4, 5, and 11
Rab 5 endosomes	48 ± 5	43 ± 8	23 ± 2	15 ± 5
	Rab4 only	Rab4 and 5	Rab4 and 11	Rab4, 5, and 11
Rab 4 endosomes, steady state/2 min + 3 min chase	24 ± 4/ND	52 ± 6/55 ± 1	50 ± 1/ND	23 ± 1/ND
Rab4 endosomes 50 nM wortmannin	ND	65.5 ± 4	34.5 ± 9	ND

Fluorescence analysis: Cells coexpressing YFP-Rab4 and CFP-Rab5 were stained with antibodies against Rab11. Numbers represent the percentage of endosomes labeled for the reference Rab protein only, or combinations of two or three Rab proteins.

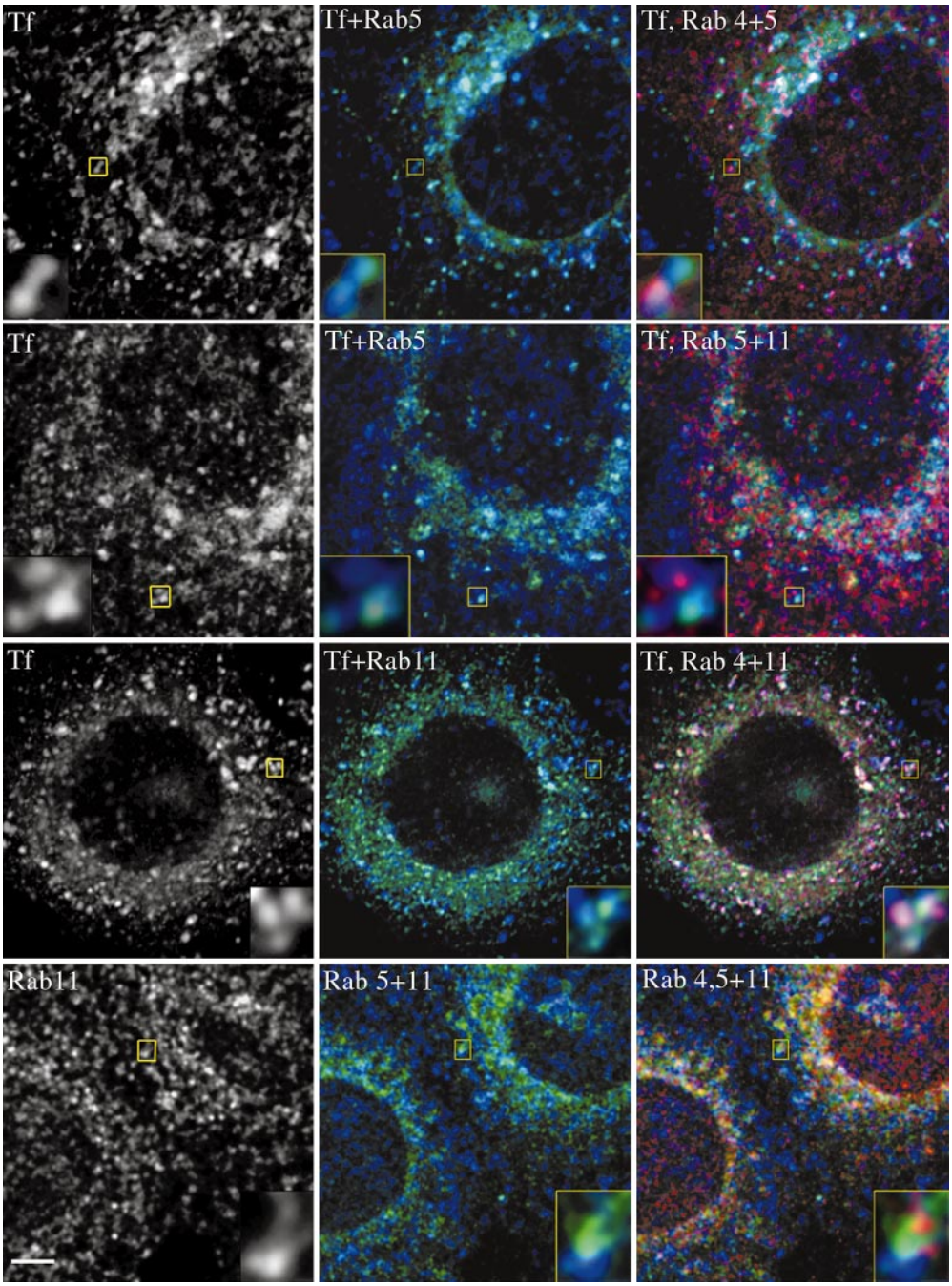

Figure 3. Confocal images of Rab4-, Rab5- and Rab11-labeling on transferrin-filled endosomes. A431 cells expressing CFP-Rab5 and YFP-Rab4 (top and bottom row), CFP-Rab5 and YFP-Rab11 (second row), CFP-Rab11 and YFP-Rab4 (third row) after internalization of Texas red transferrin for 30 min (top three rows), or staining with antibodies for Rab11 followed by secondary antibodies conjugated to Texas red (bottom row). Individual confocal sections are shown. Bar, 2 μm.

mostly found in membranes containing Rab4 and Rab11. However, it has to be noted that endosomes containing all three Rab proteins were observed, and likewise membranes containing only Rab4, only Rab11, or Rab5 and Rab11 (Tables I–III). It will probably be necessary to consider all possible combinations of domain arrangements to get a complete view of the pathway.

Electron Microscopy Confirms that Rab Proteins Localize to Distinct Membrane Domains on the Same Endosome

The data presented so far support our model for a domain organization of endosomal membranes. However, the size of the observed structures is at the limit of resolution for light microscopy techniques. We therefore sought to substantiate these findings by electron microscopy. To have the entire surface area available for immunolabeling, we decided to avoid sectioning of the membranes. Cells expressing GFP-Rab4 (Fig. 4, A and B) or GFP-Rab5 (Fig. 4 D) were incubated with 5-nm gold-conjugated to BSA for 30 min at 37°C. Membranes from postnuclear supernatants of these cells were adsorbed to copper grids by incubation at room temperature in the presence of an ATP-regenerating system and GTP. The material was labeled with antibodies to GFP and EEA1 or Rab11.

Remarkably, the gold labeling for individual Rab proteins was often localized in discrete patches (Fig. 4, A and

Table III. Quantitation of Rab4, Rab11, and EEA1 on BSA-Gold-filled Endosomes

	EEA1	Rab4	Overlap
BSA-gold endosomes, 5 min internalization	68	61	49
	Rab11	Rab4	Overlap
BSA-gold endosomes, 5 min internalization	23	59	18
BSA-gold endosomes, 30 min internalization	43	51	33
Rab4 endosomes	54	–	–

EM analysis: BSA-gold–filled endosomes from cells expressing GFP-Rab4 were immuno-labeled with antibodies against GFP and EEA1 or Rab11. Numbers represent the percentage of total BSA-gold–filled endosomes labeling for EEA1, Rab4 and Rab11, or the percentage of Rab4-positive endosomes labeling for Rab11 (bottom row).

B). These were only found on the membranes and were not observed when the material was adsorbed at 4°C (Fig. 4 C), excluding artifacts generated by protein A aggregates or overexpression of the GFP fusion proteins. However, we cannot rule out that in some instances these patches appeared particularly tight due to a collapsing of membrane elements during the staining procedure. Nevertheless, labeling for GFP-Rab4 (Fig. 4 A, arrowheads) and the Rab5 effector EEA1 (Fig. 4 A, arrows) were clearly segregated on the same endosomal membrane, as defined by the internalized BSA-gold (asterisks). Likewise, patches of endogenous Rab11, detected by an affinity-purified antibody (Fig. 4 B, arrows), were distinct from GFP-Rab4–labeled areas (Fig. 4 B, arrowheads). In contrast, both Rab5 and its effector EEA1 were localized to the same domains on endosomes from GFP-Rab5–expressing cells (Fig. 4 D, arrows). 54% of the BSA-gold–filled endosomes positive for Rab4 also labeled for Rab11 (Table III). After short internalization for 5 min, 18% of the BSA-gold–filled endosomes labeled for Rab4 and Rab11, whereas 49% contained EEA1 and Rab4 (Table III).

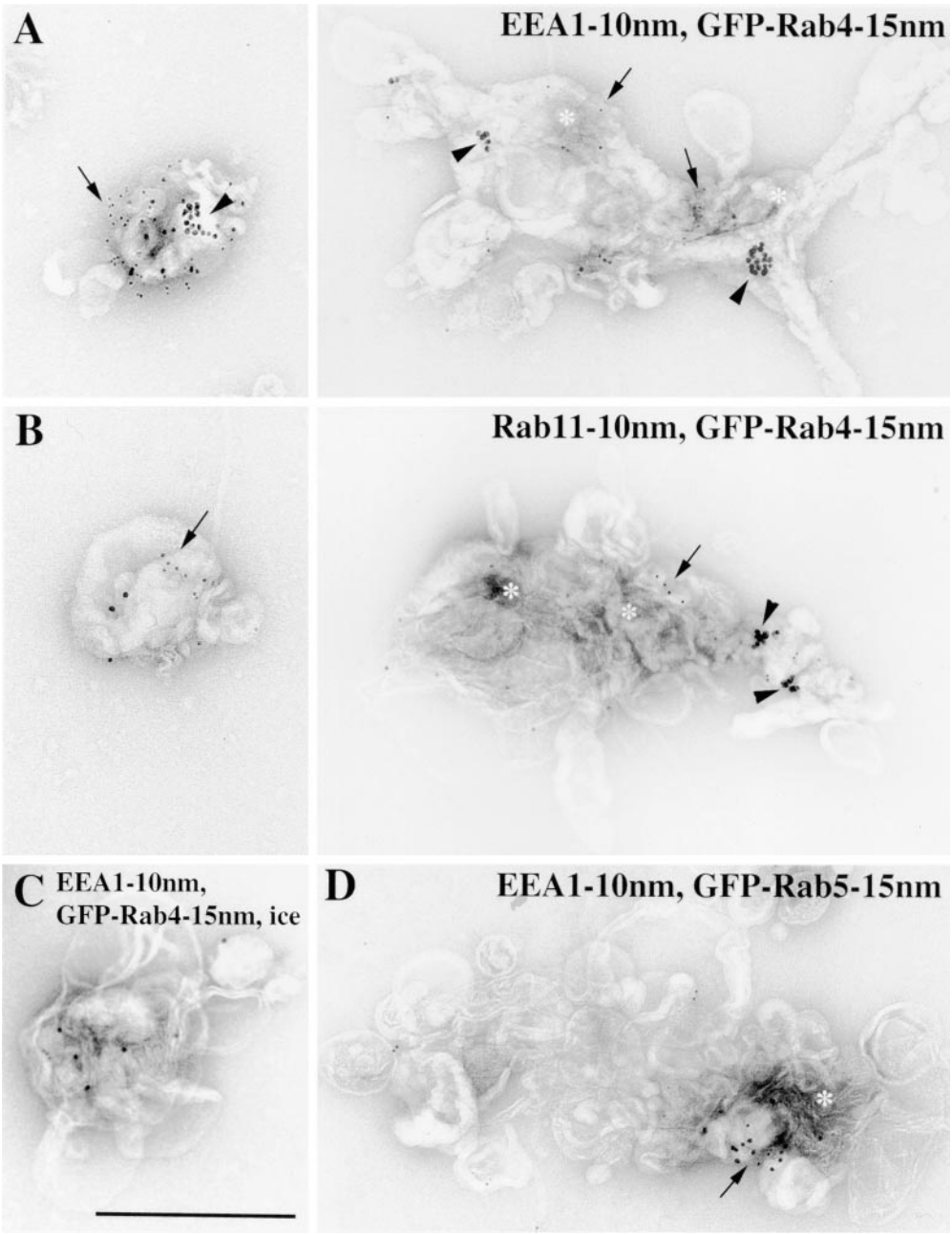

Figure 4. Distinct membrane domains of Rab4, Rab5, and Rab11 visualized by electron microscopy. A431 cells stably expressing GFP-Rab4 (A, B, and C) or GFP-Rab5 (D) were incubated with BSA coupled to 5-nm gold for 30 min at 37°C. Membranes from post nuclear supernatants were allowed to adsorb onto copper grids in the presence of an ATP-regenerating system and GTP at room temperature (A, B, and D) or on ice (C). Specimens were labeled with antibodies against EEA1 and GFP (A, C, and D) or Rab11 and GFP (B).

These numbers are consistent with the data obtained from the confocal images (Tables I and II). In summary, the ultrastructural analysis confirmed that Rab proteins and their effectors can form discrete domains on continuous membranes.

Arrangements of Distinct Membrane Domains within the Same Endosome Can Be Visualized in Living Cells

In a third approach, we studied the proposed domain organization in living cells, following Rab4, Rab5, and Rab11, coexpressed as YFP and CFP fusion proteins, by time-lapse video microscopy. As expected, the labeled endosomes were highly dynamic. Nevertheless, following individual structures over time, we frequently observed that more than one type of Rab protein occupied continuous membrane elements. More importantly, also in living cells, fluorescent signals were mostly segregated within the same structure (Fig. 5 A and videos 4–6). This was not a consequence of the imaging technique since in cells coexpressing YFP-Rab11 and CFP-Rab11, both signals were clearly overlapping (not shown). As in fixed cells, we mainly found Rab4 and Rab5, or Rab4 and Rab11 residing on the same endosome (Fig. 5 A). Rab5 was restricted to globular domains, which in some instances could be observed to dock or fuse (Fig. 5 A, middle panel, arrows, and video 5). Parts of the Rab4 domain on Rab5-positive endosomes were often seen to segregate into distinct tubular or vesicular structures (arrows, top panel, and video 4). Similar observations were made for endosomes containing Rab4 and Rab11, both proteins entering separate tubules and vesicles (Fig. 5, bottom panel, arrows). Thus, Rab domains are not generated by fixation but can be observed in living cells.

Domains on Rab4 and Rab11 Endosomes Are Sensitive to Brefeldin A

We next asked whether structural alterations on the endosomal membrane would perturb the segregation of Rab4, Rab5, and Rab11. Transferrin and Rab4 have been shown to localize to an extensive tubular network in response to brefeldin A (BFA; Tooze and Hollinshead, 1992; Daro et al., 1996). Consistently, we found that transferrin rapidly entered long GFP-Rab4–positive tubules after a short treatment with BFA (Fig. 5 B and video 7). In cells expressing CFP-Rab11 and YFP-Rab4 both proteins localized to the same tubular network (Fig. 5 B, arrows, and video 8), but were no longer clearly segregated in distinct domains. Remarkably, a fraction of Rab4-containing endosomes did not form tubules, but rather remained in distinct globular structures. These membranes contained little or no Rab11 (Fig. 5 B, arrowheads). Imaging cells expressing CFP-Rab5 and YFP-Rab4 under these conditions revealed that Rab5-positive endosomes were resistant to BFA-induced tubulation. Likewise, Rab4 remained in the globular part when present on Rab5 endosomes (Fig. 5 B and video 9). The amount of Rab4 on Rab5-positive membranes was slightly decreased compared with control cells (30 ± 8% vs. 43 ± 6%), suggesting that some Rab4 entered the tubular network from Rab5-positive endosomes.

Consistent with this observation, transit of transferrin from Rab4/Rab5-positive endosomes to the Rab4/Rab11 network proceeded when cells were pretreated with BFA to allow tubule formation. Rhodamine transferrin, internalized for 2 min at 37°C, was followed by a chase in the presence of BFA (Fig. 6). The amount of Rab5-positive transferrin structures was slightly higher than in control cells at early time points (Fig. 6 A), however, we found no significant morphological difference to nontreated cells (Fig. 6 B, Rab5 panel, compare with Fig. 2 B). Transfer of transferrin into Rab4-labeled endosomes proceeded faster in the presence of BFA (Fig. 6 A, 2 min), but at early stages the cargo remained restricted to globular Rab4-positive endosomes and was largely excluded from the tubular network (Fig. 6 B). After 5 min, transferrin had left Rab5 positive and reached Rab4-labeled membranes to similar levels as seen in control cells (Fig. 6 A). At this point some cargo had entered the BFA-induced tubular network (Fig. 6 B). This was accompanied by a slight increase for Rab11 labeling compared with nontreated cells, consistent with the observation that Rab4 and Rab11 were not clearly segregated in these tubules. At later time points most of the transferrin was found in a membrane network that did not permit quantitation of individual structures (not shown).

Given that recycling is only marginally effected by BFA (Lippincott-Schwartz et al., 1991; our unpublished data), the bulk of transferrin might be delivered back to the surface directly from the BFA resistant Rab5/Rab4 endosomes. However, segregation of Rab4 and Rab11 domains might not be strictly required, and recycling could occur after a fast transit into the tubular network.

Wortmannin Treatment Delays Exit of Transferrin from Rab4/Rab5-Positive Endosomes

Cells treated with the phosphatidylinositol-kinase inhibitor wortmannin show a delay in transferrin recycling (Spiro et al., 1996). The activity of the PI-(3)-kinase hVPS34 is necessary for the membrane recruitment of the Rab5 effector EEA1 (Mills et al., 1998; Simonsen et al., 1998; Christoforidis, et al., 1999b), suggesting that a Rab5 domain requires a microenvironment of PI(3)P and active Rab5 with its effectors on the membrane. Therefore, depletion of PI(3)P by wortmannin treatment should perturb the Rab5 domain. To test whether this might interfere with the transfer of transferrin to Rab4-positive domains, we quantitated the codistribution of Rab4, Rab5, and Rab11 with transferrin after 30 min internalization in the presence of 50 nm wortmannin (Table I). Consistent with our hypothesis, we found that compared with control cells twice as many transferrin-labeled endosomes contained Rab4 and Rab5 (47 ± 14% vs. 23 ± 7%, Table I). Likewise, the number of cargo-filled structures containing Rab4 and Rab11 was reduced to almost half compared with control cells (35 ± 6% vs. 63.5 ± 5%, Table I), indicating that transferrin was retained in Rab4/Rab5 endosomes upon wortmannin treatment. Moreover, also the domain arrangement was changed as judged by the number of Rab4-positive endosomes containing either Rab5 or Rab11. More Rab4 endosomes were positive for Rab5 (65.5 ± 4% vs. 52 ± 6%) and fewer labeled for Rab11 (34.5 ± 9% vs. 50 ± 1%, Table II). Sorting of membrane associated cargo has been suggested to occur by segrega-

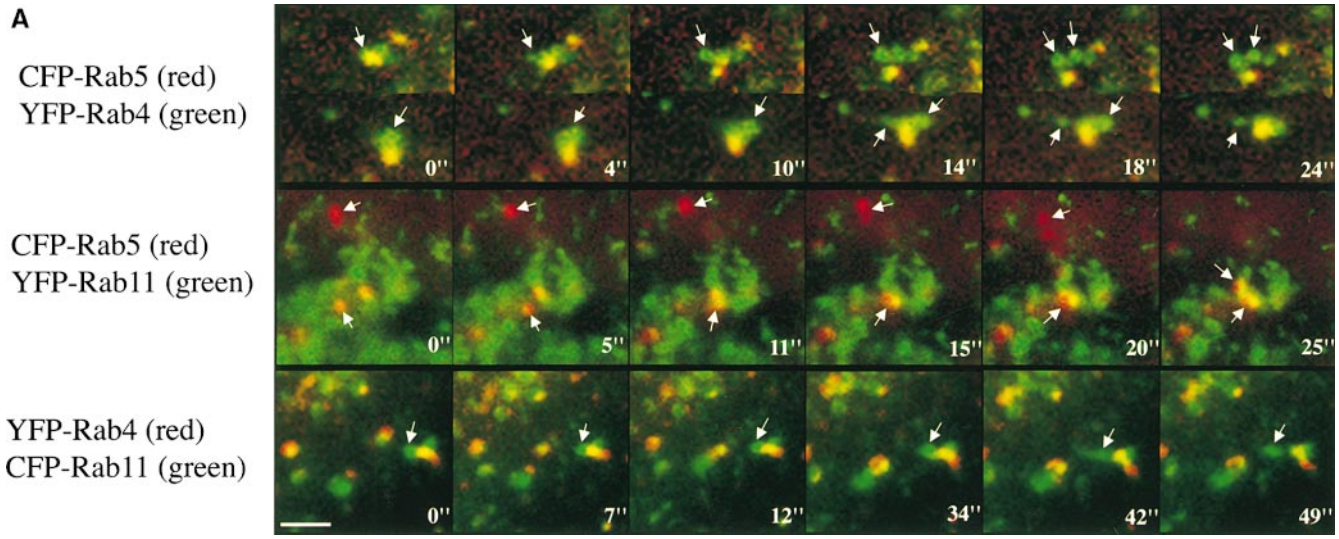

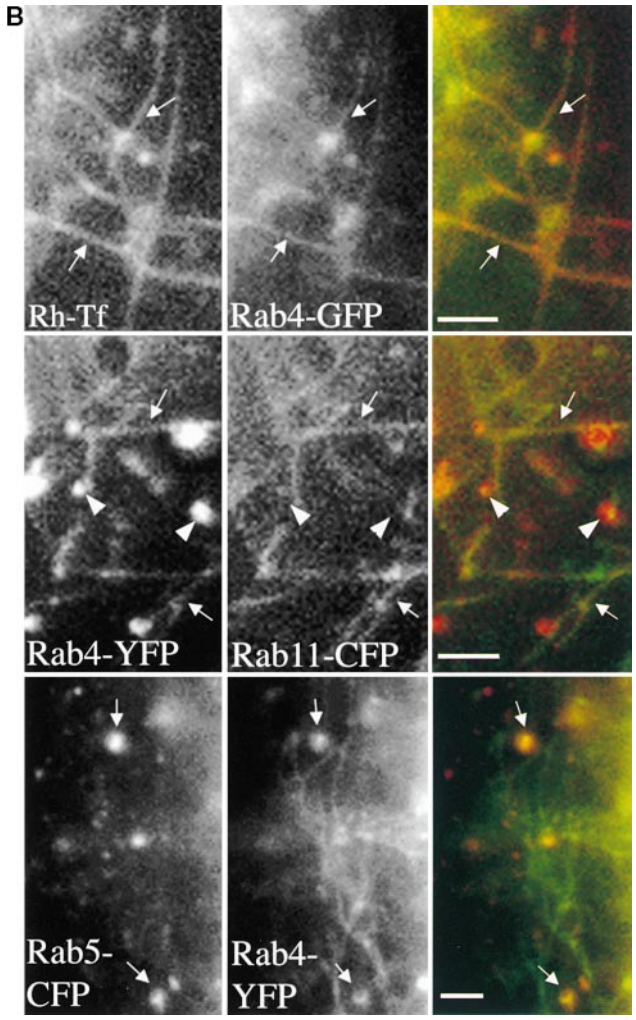

Figure 5. Visualization of Rab proteins on endosomal membrane domains by time-lapse video microscopy. (A) Time-lapse series of A431 cells coexpressing CFP and YFP fusion proteins of Rab4, Rab5, and Rab11. (B) Differential response of Rab4, Rab5, and Rab11 membrane domains to treatment with BFA. Single frames from time-lapse series (compare videos 4–6). (Top) Cells expressing GFP-Rab4 after internalization of rhodamine transferrin for 10 min followed by treatment with 5 μg/ml BFA for 10 min. (Middle and bottom) Cells expressing combinations of Rab4 and Rab11, or Rab4 and Rab5. Bars: (A) 1 μm; (B) 1 μm.

tion from globular into tubular domains of the endosome (Mayor et al., 1993). The observed delay of transferrin recycling in wortmannin-treated cells might be explained by the perturbation of this domain structure. Consistently, wortmannin treatment frequently resulted in structural changes of Rab5 endosomes (video 10), which were not observed on Rab11 membranes.

Discussion

Although endocytosis and receptor recycling have been extensively studied, the compartmental organization of endosomes is still poorly understood. The small GTPases Rab4, Rab5, and Rab11 are well-accepted regulators of the endocytic/recycling pathway (Bucci et al., 1992; Van der Sluijs et al., 1992; Ullrich et al., 1996; Ren et al., 1998). To test whether these Rab proteins can functionally arrange membrane domains within the same organelle, we have visualized Rab4, Rab5, and Rab11 on cargo-filled endosomes by video, confocal, and electron microscopy. Three principle conclusions can be drawn from this study. First, Rab proteins are localized in morphologically distinct domains, which can reside on the same endosome. Second, these membrane domains are dynamic but do not significantly intermix over time. Furthermore, the overall distribution of Rab4, Rab5, and Rab11 domains on endosomes does not significantly change at different stages of recycling. Third, endosomes comprised of different domain arrangements display differential pharmacological sensitivity, reflecting their biochemical and possibly functional diversity. On the basis of these results, we propose a model that describes endosomes as a mosaic of functional membrane domains (Fig. 7). These domains would be organized by Rab proteins and similar regulatory proteins through local recruitment of specific effector proteins. Therefore, it is the nature of the effector molecules that specifies the function(s) of a domain. To coordinate various functions, different domains would communicate, possibly via effectors shared between neighboring Rab proteins.

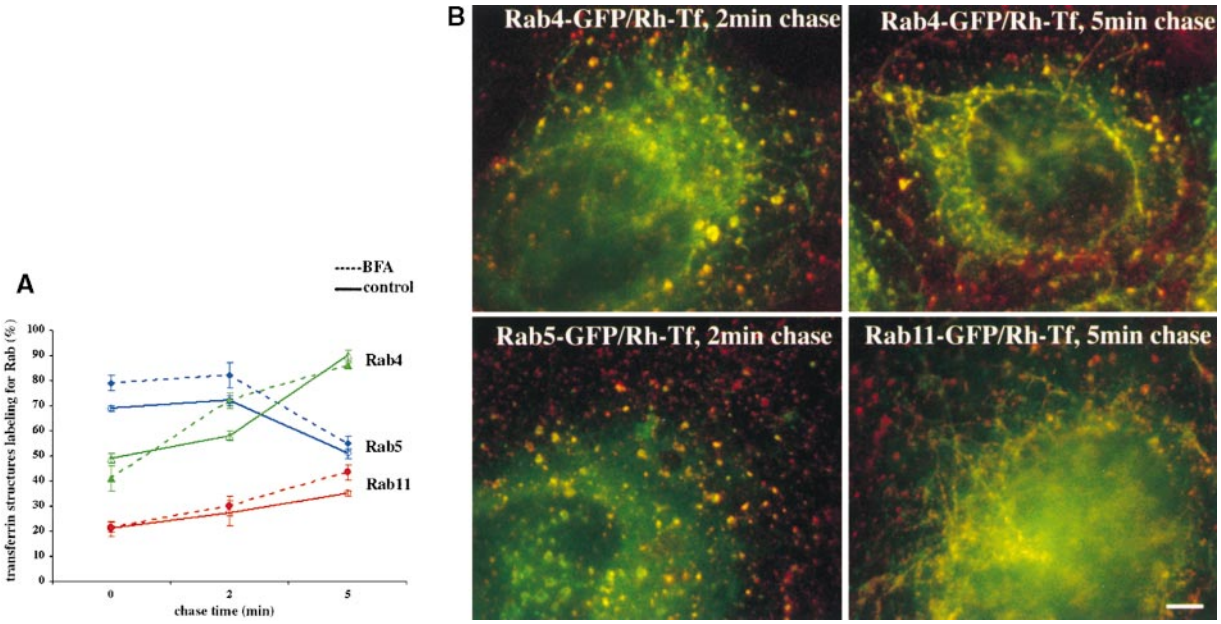

Figure 6. Transfer of transferrin from Rab4/Rab5 to Rab4/Rab11-positive endosomes proceeds in BFA-treated cells. (A) A431 cells stably expressing GFP-Rab4, -Rab5, or -Rab11 were labeled with rhodamine transferrin for 2 min followed by a chase for the indicated time points. BFA treatment of the cells was started 5 min before and continued during internalization and chase times. For acquisition and quantitation of the fluorescent images see Fig. 2 and Materials and Methods. (B) Representative merged images for BFA-treated cells (compare with Fig. 2 B). Bar, 2 μm.

Targeting of the GFP fusion proteins, their accessibility to Rab GDI, and the kinetics of transferrin recycling indicate that the experimental strategy we have chosen allows the faithful visualization of endosomal organelles. Quantitation of the confocal images showed that transferrin enters via structures containing mainly Rab5, consistent with the fact that Rab5 is found on clathrin-coated vesicles and required for docking and fusion of these with early endosomes (Bucci et al., 1992; Horiuchi et al., 1995; McLauchlan et al., 1998). Fast recycling coincided with transferrin localization in Rab4/Rab5-positive endosomes, whereas at steady state transferrin accumulated in Rab4/Rab11 containing membranes. Concerning the overall distribution of the Rab proteins, our morphological quantifications are in agreement with previous biochemical studies. With an immunoisolation approach, Trischler et al. (1999) identified endosome populations with the same extent of overlap between Rab4, Rab5, and Rab11. Sheff et al. (1999) obtained similar results using a gradient fractionation technique. More importantly, the morphological approach provided insights into the spatial organization of the Rab proteins. When visualized by video microscopy of living cells, confocal microscopy, and electron microscopy, different Rab proteins are segregated into distinct domains on the same membrane, presumably stabilized by their effectors. Since the overall distribution of Rab4, Rab5, and Rab11 does not change with the flow of cargo, the data support the interpretation that Rab proteins belong to the intrinsic structural and functional machinery of endosomes. This has important consequences for the definition of organelles in the recycling pathway. With respect to Rab proteins, both early and recycling endosomes are

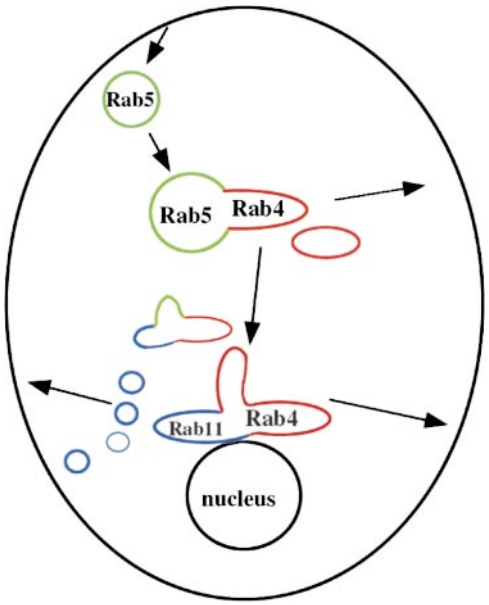

Figure 7. Model, describing endocytic organelles as a mosaic of membrane domains. The domain distribution of the three Rab proteins presented in this study, Rab4, Rab5, and Rab11 is depicted in red, green, and blue, respectively. Compartmentalization is achieved by dynamic functional arrangements of these domains, combinations of Rab4 and Rab5, and Rab4 and Rab11 being the most abundant. Arrows indicate direction of transferrin recycling. Cargo enters the cell via mainly Rab5-containing structures. Fast recycling is achieved by rapid sorting from Rab5 into Rab4-positive domains on the same endosome. Recycling slows down once transferrin enters pericentriolar membranes dominated by Rab4 and Rab11 domains.

structured into Rab4, Rab5, and Rab11 domains, only the relative amounts of these domains differ. Early endosomes in the cell periphery are primarily composed of Rab5 and Rab4 domains and contain few Rab11 domains. Conversely, recycling endosomes in the pericentriolar area mainly contain Rab4 and Rab11 domains (Fig. 7). Whether the same effector proteins bind to a particular Rab protein, regardless of where the domain is located, remains to be investigated. The idea that this domain organization can create a biochemically distinct environment is supported by the differential effects of wortmannin and BFA. It should be noted, that several other Rab proteins are localized on endosomes (Olkkonen et al., 1993; Lütcke et al., 1994). Moreover, in all likelihood the Rab machineries cooperate with other regulatory molecules (e.g., ARF and ARF effectors, see below) to create platforms for membrane organization. Consequently, a variety of endosomal subpopulations may arise from combinatorial arrangements of individual domains.

How then is efficient receptor recycling achieved? By mathematical modeling the transferrin route is best described assuming two recycling stations with different kinetic properties (Sheff et al., 1999). The first is filled maximally within 5 min, subsequently more than two-thirds of the remaining transferrin will accumulate in the second station after 25 min. Our data would imply a role for Rab4 on both of these sorting stations. 90% of the transferrin was associated with Rab4-positive endosomes at early time points, and 64% of the transferrin was found in Rab4 and Rab11-positive endosomes after 30 min of internalization. Fast recycling seems to require a rapid sorting of transferrin from a Rab5 into a Rab4 domain on the same endosome. This process is delayed when the Rab5 domain is perturbed by wortmannin treatment. One could envisage that neighboring domains would communicate via common effector proteins. One such candidate protein would be rabaptin5 (Vitale et al., 1998), which binds both Rab4 and Rab5. Once transferrin has traversed Rab5/Rab4 endosomes, it would accumulate in membranes enriched for Rab4 and Rab11 domains. These membranes would exert slower kinetics of recycling and exhibit different sorting capacity. Whereas the role for Rab5 in endosome fusion is well established, the exact functions of Rab4 and Rab11 are unknown. These two GTPases might be directly involved in the formation of recycling vesicles, possibly targeted to different sites of the plasma membrane. For example, Rab11 might have a role in polarized transport in epithelial or motile cells (e.g., facilitate transcytosis of cargo like the polymeric IgA receptor; Sheff et al., 1999), whereas Rab4 would regulate a more general route of membrane recycling. The nature of the recycling vesicles is unclear. Coated buds have been observed on tubulovesicular endosomes (Stoorvogel et al., 1996), and the tubulation of Rab4/Rab11 membranes upon BFA treatment is most likely due to the inhibition of ARF-dependent processes (Donaldson et al., 1992; Helms and Rothman, 1992). However, whether coated vesicles actively participate in recycling remains to be established. If sorting is completed once transferrin has reached a Rab4-positive domain, coat assembly might not be absolutely required. Alternatively, a BFA-insensitive exchange factor for ARF might exist on Rab4/Rab5 endosomes. Either mechanism would explain why recycling is only marginally effected by BFA.

In summary, envisaging endosomes as dynamic arrangements of membrane domains can give an integrative view on the complexity and robustness of the recycling pathway. This model not only agrees with the observed kinetics (Sheff et al., 1999), but also explains how in some cell types a seemingly continuous membrane system can achieve compartmentalization (Hopkins et al., 1990). However, at the molecular level it is mainly based on the interactions of a single Rab protein, Rab5, with its effectors. Besides the morphological evidence reported here, to show that these domains generally serve as a platform for membrane organization, it will be necessary to characterize Rab4 and Rab11 effector proteins. This is now the focus of our attention.

We are grateful to Drs. Ponnambalam, Le Bot, and Stenmark for kindly providing antibodies. We would also like to thank A. Habermann for technical assistance with electron microscopy and A. Atzberger for FACS® analysis of the GFP cell lines. Olympus and TILL Photonics generously provided equipment and support to the Advanced Light Microscopy Facility at EMBL. Special thanks to G. Griffith, K. Simons, and H. McBride for critical reading of the manuscript and helpful comments.

B. Sönnichsen and E. Nielsen were supported by long term European Molecular Biology Organization fellowships. This work was supported by the Max Planck Society and grants from the Human Frontier Science Program (RG-432/96), European Union Training and Mobility of Researchers (ERB-CT96-0020), and Biomed (BMH4-97-2410; M. Zerial).

Submitted: 17 February 2000
Revised: 28 March 2000
Accepted: 10 April 2000

References

Besterman, J.M., H.A. Airhart, R.C. Woodworth, and R.B. Low. 1981. Exocytosis of pinocytosed fluid in cultured cells: kinetic evidence for rapid turnover and compartmentation. *J. Cell Biol.* 91:716–727.

Brown, H.A., S. Gutowski, C.R. Moomaw, C. Slaughter, and P.C. Sternweis. 1993. ADP-ribosylation factor, a small GTP-dependent regulatory protein stimulates phospholipase D activity. *Cell.* 75:1137–1144.

Bucci, C., R.G. Parton, I.H. Mather, H. Stunnenberg, K. Simons, B. Hoflack, and M. Zerial. 1992. The small GTPase rab5 functions as a regulatory factor in the early endocytic pathway. *Cell.* 70:715–728.

Calhoun, B.C., L.A. Lapierre, C.S. Chew, and J.R. Goldenring. 1998. Rab11a redistributes to apical secretory canaliculus during stimulation of gastric parietal cells. *Am. J. Physiol.* 275:C163–C170.

Chen, W., Y. Feng, D. Chen, and A. Wandinger-Ness. 1998. Rab11 is required for trans-Golgi network-to-plasma membrane transport and a preferential target for GDP dissociation inhibitor. *Mol. Biol. Cell.* 9:3241–3257.

Christoforidis, S., H.M. McBride, R.D. Burgoyne, and M. Zerial. 1999a. The Rab5 effector EEA1 is a core component of endosome docking and fusion. *Nature.* 397:621–625.

Christoforidis, S., M. Miaczynska, K. Ashman, M. Wilm, L. Zhao, S.-C. Yip, M.D. Waterfield, J.M. Backer, and M. Zerial. 1999b. Phosphoinositide-3-kinases are Rab5 effectors. *Nat. Cell Biol.* 4:249–252.

Daro, E.P., P. van der Sluijs, T. Galli, and I. Mellman. 1996. Rab4 and cellubrevin define different early endosome populations on the pathway of transferrin receptor recycling. *Proc. Natl. Acad. Sci. USA.* 93:9559–9564.

Donaldson, J.G., D. Finazzi, and R.D. Klausner. 1992. Brefeldin A inhibits Golgi membrane-catalyzed exchange of guanine nucleotide onto ARF protein. *Nature.* 360:350–352.

Dunn, K.W., T.E. McGraw, and F.R. Maxfield. 1989. Iterative fractionation of recycling receptors from lysosomally destined ligands in an early sorting endosome. *J. Cell Biol.* 109:3303–3314.

Echard, A., F. Jollivet, O. Martinez, J.J. Lacapere, A. Rousselet, I. Janoueix-Lerosey, and B. Goud. 1998. Interaction of a Golgi-associated kinesin-like protein with Rab6. *Science.* 279:580–585.

Ghosh, R.N., D.L. Gelman, and F.R. Maxfield. 1994. Quantification of low-density lipoprotein and transferrin endocytic sorting in Hep2 cells. *J. Cell Biol.* 128:549–561.

Ghosh, R.N., W.G. Mallet, T.T. Soe, T.E. McGraw, and F.R. Maxfield. 1998. An endocytosed TGN38 chimeric protein is delivered to the TGN after trafficking through the endocytic recycling compartment in CHO cells. *J. Cell*

Biol. 142:923–936.
Gorvel, J.P., P. Chavrier, M. Zerial, and J. Gruenberg. 1991. Rab5 controls early endosome fusion in vitro. *Cell*. 64:915–925.
Griffiths, G., R. Back, and M. Marsh. 1989. A quantitative analysis of the endocytic pathway in baby hamster kidney cells. *J. Cell Biol.* 109:2703–2720.
Gruenberg, J., and F.R. Maxfield. 1995. Membrane transport in the endocytic pathway. *Curr. Opin. Cell Biol.* 7:552–563.
Guo, W., D. Roth, C. Walch-Solimena, and P. Novick. 1999. The exocyst is an effector for Sec4p, targeting secretory vesicles to sites of exocytosis. *EMBO (Eur. Mol. Biol. Organ.) J.* 18:1071–1080.
Helms, J.B., and J.E. Rothman. 1992. Inhibition by brefeldin-A of a Golgi membrane enzyme that catalyzes exchange of guanine-nucleotide bound to ARF. *Nature*. 360:352–354.
Hopkins, C.R. 1983. Intracellular routing of transferrin and transferrin receptors in epidermoid carcinoma A431 cells. *Cell*. 35:321–330.
Hopkins, C.R., A. Gibson, M. Shipman, and K. Miller. 1990. Movement of internalized ligand-receptor complexes along a continuous endosomal reticulum. *Nature*. 346:335–339.
Horiuchi, H., A. Giner, B. Hoflack, and M. Zerial. 1995. A GDP/GTP exchange-stimulatory activity for the Rab5–RabGDI complex on clathrin-coated vesicles from bovine brain. *J. Biol. Chem*. 270:11257–11262.
Horiuchi, H., R. Lippé, H.M. McBride, M. Rubino, P. Woodman, H. Stenmark, V. Rybin, M. Wilm, K. Ashman, M. Mann, and M. Zerial. 1997. A novel Rab5 GDP/GTP exchange factor complexed to Rabaptin-5 links nucleotide exchange to effector recruitment and function. *Cell*. 90:1149–1159.
Jedd, G., J. Mulholland, and N. Segev. 1997. Two new ypt GTPases are required for exit from the yeast trans-golgi compartment. *J. Cell Biol*. 137:563–580.
Lippincott-Schwartz, J., L. Yuan, C. Tipper, M. Amherdt, L. Orci, and R.D. Klausner. 1991. Brefeldin A's effects on endosomes, lysosomes, and the TGN suggest a general mechanism for regulating organelle structure and membrane traffic. *Cell*. 67:601–616.
Lütcke, A., A. Valencia, V. Olkkonen, P. Dupree, R.G. Parton, K. Simons, and M. Zerial. 1994. Cloning and subcellular localization of novel rab proteins reveals polarized and cell-type specific expression. *J. Cell Sci.* 107: 3437–3448.
Mayor, S., J.F. Presley, and F.R. Maxfield. 1993. Sorting of membrane components from endosomes and subsequent recycling to the cell surface occurs by a bulk flow process. *J. Cell Biol*. 121:1257–1269.
McBride, H.M., V. Rybin, C. Murphy, A. Giner, R. Teasdale, and M. Zerial. 1999. Oligomeric complexes link Rab5 effectors with NSF and drive membrane fusion via interactions between EEA1 and syntaxin13. *Cell*. 98:377–386.
McLauchlan, H., J. Newell, N. Morrice, A. Osborne, M. West, and E. Smythe. 1998. A novel role for Rab5-GDI in ligand sequestration into clathrin-coated pits. *Curr. Biol*. 8:34–45.
Mellman, I. 1996. Endocytosis and molecular sorting. *Annu. Rev. Cell Dev. Biol.* 12:575–625.
Mills, I.G., A.T. Jones, and M.J. Clague. 1998. Involvement of the endosomal autoantigen EEA1 in homotypic fusion of early endosomes. *Curr. Biol.* 8:881–884.
Mu, F.T., J.M. Callighan, O. Steele-Mortimer, H. Stenmark, R.G. Parton, P.L. Campbell, J. McCluskey, J.P. Yeo, E.P.C. Tock, and B.-H. Toh. 1995. EEA1, an early endosome-associated protein. *J. Biol. Chem*. 270:13503–13511.
Nielsen, E., F. Severin, J.M. Backer, A.A. Hyman, and M. Zerial. 1999. Rab5 regulates motility of early endosomes on microtubules. *Nat. Cell Biol.* 1:376–382.
Novick, P., and M. Zerial. 1997. The diversity of Rab proteins in vesicle transport. *Curr. Opin. Cell Biol.* 9:496–504.
Olkkonen, V.M., P. Dupree, I. Killisch, A. Lutcke, M. Zerial, and K. Simons. 1993. Molecular cloning and subcellular localization of 3 GTP-binding proteins of the rab subfamily. *J. Cell Sci.* 106:1249–1261.
Patki, V., J. Virbasius, W.S. Lane, B.-H. Toh, H.S. Shpetner, and S. Corvera. 1997. Identification of an early endosomal protein regulated by phosphatidylinositol 3-kinase. *Proc. Natl. Acad. Sci. USA*. 94:7326–7330.
Pfeffer, S.R. 1994. Rab GTPases: master regulators of membrane trafficking. *Curr. Opin. Cell Biol.* 6:522–526.
Ren, M., G. Xu, J. Zeng, C. De Lemos-Chiarandini, M. Adesnik, and D.D. Sabatini. 1998. Hydrolysis of GTP on rab11 is required for the direct delivery of transferrin from the pericentriolar recycling compartment to the cell surface but not from sorting endosomes. *Proc. Natl. Acad. Sci. USA*. 95:6187–6192.
Schmid, S.L., R. Fuchs, P. Male, and I. Mellman. 1988. Two distinct subpopulations of endosomes involved in membrane recycling and transport to lysosomes. *Cell*. 52:73–83.
Schu, P.V., K. Takegawa, M.J. Fry, J.H. Stack, M.D. Waterfield, and S.D. Emr. 1993. Phosphatidylinositol 3-kinase encoded by yeast VPS34 gene essential for protein sorting. *Science*. 260:88–91.
Sheff, D.R., E.A. Daro, M. Hull, and I. Mellman. 1999. The recycling pathway contains two distinct populations of early endosomes with different sorting functions. *J. Cell Biol.* 145:123–139.
Simonsen, A., R. Lippé, S. Christoforidis, J.-M. Gaullier, A. Brech, J. Callaghan, B.-H. Toh, C. Murphy, M. Zerial, and H. Stenmark. 1998. EEA1 links phosphatidylinositol 3-kinase function to Rab5 regulation of endosome fusion. *Nature*. 394:494–498.
Sipe, D.M., and R.F. Murphy. 1987. High resolution acidification kinetics of transferrin in Balb/c 3T3 cells: exposure to pH 6 followed by temperature-sensitive alkalization during recycling. *Proc. Natl. Acad. Sci. USA*. 84:7119–7125.
Spiro, D.J., W. Boll, T. Kirchhausen, and M. Wessling-Resnick. 1996. Wortmannin alters the transferrin receptor endocytic pathway in vivo and in vitro. *Mol. Biol. Cell*. 7:355–367.
Stoorvogel, W., V. Oorschot, and H.J. Geuze. 1996. A novel class of clathrin-coated vesicles budding from endosomes. *J. Cell Biol*. 132:21–33.
Tooze, J., and M. Hollinshead. 1992. In AtT20 and HeLa cells brefeldin A induces the fusion of tubular endosomes and changes their distribution and some of their endocytic properties. *J. Cell Biol.* 118:813–830.
Trischler, M., W. Stoorvogel, and O. Ullrich. 1999. Biochemical analysis of distinct Rab5- and Rab11-positive endosomes along the transferrin pathway. *J. Cell Sci.* 112:4773–4783.
Ullrich, O., S. Reinsch, S. Urbé, M. Zerial, and R.G. Parton. 1996. Rab11 regulates recycling through the pericentriolar recycling endosome. *J. Cell Biol.* 135:913–924.
Urbe, S., L.A. Huber, M. Zerial, S.A. Tooze, and R.G. Parton. 1993. Rab11, a small GTPase associated with both constitutive and regulated secretory pathways in PC12 cells. *FEBS Lett.* 334:175–182.
Van der Sluijs, P., M. Hull, P. Webster, P. Mâle, B. Goud, and I. Mellman. 1992. The small GTP-binding protein rab4 controls an early sorting event on the endocytic pathway. *Cell*. 70:729–740.
Vitale, G., V. Rybin, S. Christoforidis, P. Thornqvist, M. McCaffrey, H. Stenmark, and M. Zerial. 1998. Distinct Rab-binding domains mediate the interaction of Rabaptin-5 with GTP-bound rab4 and rab5. *EMBO (Eur. Mol. Biol. Organ.) J.* 17:1941–1951.
White, J., B. Storie, S. Rötger, E.H.K. Stelzer, T. Suganuma, and T. Nilsson. 1998. Recycling of Golgi resident glycosyltransferases through the ER reveals a novel pathway and provides an explanation for nocodazole-induced Golgi scattering. *J. Cell Biol.* 143:1505–1521.
Yamashiro, D.J., and F.R. Maxfield. 1984. Segregation of transferrin to a mildly acidic (pH 6.5) para-Golgi compartment in the recycling pathway. *Cell*. 37: 789–800.
Zacchi, P., H. Stenmark, R.G. Parton, D. Orioli, F. Lim, A. Giner, I. Mellman, M. Zerial, and C. Murphy. 1998. Rab17 regulates membrane trafficking through apical recycling endosomes in polarized epithelial cells. *J. Cell Biol.* 140:1039–1053.